

Electronic inhomogeneity of heavily overdoped $\text{Bi}_{2-x}\text{Pb}_x\text{Sr}_2\text{CuO}_y$ studied by low-temperature scanning tunneling microscopy/spectroscopy

H. Mashima, N. Fukuo, and Y. Matsumoto

Frontier Collaborative Research Center, Tokyo Institute of Technology, 4259 Nagatsutacho, Midori-ku, Yokohama 226-8503, Japan

G. Kinoda

Kanagawa Academy of Science and Technology, 3-2-1 Sakado, Takatsu-ku, Kawasaki 213-0012, Japan

T. Kondo and H. Ikuta

Department of Crystalline Materials Science, Nagoya University, Furocho, Chikusa-ku, Nagoya 464-8603, Japan

T. Hitosugi and T. Hasegawa

Department of Chemistry, University of Tokyo, 7-3-1 Hongo, Bunkyo-ku, Tokyo 113-0033, Japan

(Received 29 September 2005; revised manuscript received 29 November 2005; published 13 February 2006)

Low-temperature scanning tunneling microscopy and/or scanning tunneling spectroscopy measurements of heavily overdoped $\text{Bi}_{2-x}\text{Pb}_x\text{Sr}_2\text{CuO}_y$ have revealed nanoscale electronic inhomogeneity composed of spatial regions showing superconducting and pseudogaplike gap structures. This proves that the inhomogeneity is a general feature of Bi-based cuprates, regardless of the number of CuO_2 planes. The magnitude of inhomogeneity, defined as relative standard deviation of the local gap value, is close to that of slightly overdoped $\text{Bi}_2\text{Sr}_2\text{CaCu}_2\text{O}_y$, suggesting that the electronic inhomogeneity arises from excess oxygen atoms in the $(\text{BiO})_2$ layers.

DOI: [10.1103/PhysRevB.73.060502](https://doi.org/10.1103/PhysRevB.73.060502)

PACS number(s): 74.72.Hs, 07.79.Cz, 74.25.Jb, 71.55.-i

Scanning tunneling microscopy and/or scanning tunneling spectroscopy (STM/STS), which is capable of directly probing the local density of states (LDOS) of a sample surface on an atomic scale, has been utilized to measure the local electronic nature of high-temperature superconductivity, including quasiparticle bound states around vortex cores,¹⁻³ magnetic and nonmagnetic impurities of Cu sites,^{4,5} and defects in the blocking layers.⁶ Furthermore, STM/STS has recently been used to highlight the granular superconductivity of Bi-based cuprates, in which superconducting domains varying over a very short length scale of the order of the coherence length coexist with the nonsuperconducting matrix, exhibiting pseudogaplike spectra.⁷⁻¹⁷ Pan *et al.*¹⁰ reported the inhomogeneity manifested as spatial variations in the local density of state (LDOS) spectrum and energy gap Δ . Lang *et al.*¹¹ used Ni impurity atoms substituted for the Cu sites as markers for local superconductivity, and found that spatial regions with $\Delta > 50$ meV are nonsuperconducting. The origin of the electronic inhomogeneity has been discussed from both experimental and theoretical viewpoints.¹⁸⁻²² On the basis of detailed analyses of the spatial variations of LDOS and Δ , Pan *et al.* linked the inhomogeneity to the unscreened Coulomb potential associated with excess oxygen atoms in the $(\text{BiO})_2$ layers.¹⁰ We reported that the Δ distribution tends to spread with oxygen annealing in the case of $\text{Bi}_{2-x}\text{Pb}_x\text{Sr}_2\text{CaCu}_2\text{O}_y$ (Pb-Bi2212),¹⁴ supporting the inhomogeneity scenario based on oxygen disorder. Theoretical studies based on t - J models incorporating the disordered Coulomb potential revealed that the ionic potential caused redistribution of the local hole density and a concomitant reduction in the d -wave order parameter.¹⁸ The calculated tunneling spectra reproduced experimentally observed fea-

tures, namely, the nanoscale variation of STM topography and the negative correlation between the local gap and integrated LDOS. These arguments lead to a conclusion that electronic inhomogeneity is inherent to high- T_c superconductivity.^{7,8,10,11,14} On the other hand, several groups reported more homogeneous LDOS²³⁻²⁵ rather suggesting that the gap distribution is not essential for the occurrence of high T_c . It should be noted that the significant gap inhomogeneity, as mentioned above, has only been observed in $\text{Bi}_2\text{Sr}_2\text{CaCu}_2\text{O}_y$ (Bi2212). For more general conclusions, other compounds with different crystallographic structures must be investigated.

Here we report the results of cryogenic STM/STS of $\text{Bi}_{2-x}\text{Pb}_x\text{Sr}_2\text{CuO}_y$ (Pb-Bi2201) single crystals. Since Bi2201 has a single CuO_2 layer per unit cell, a comparison of STS results between Bi2201 and Bi2212 is expected to answer the intriguing question of how the number of CuO_2 layers influences the electronic inhomogeneity in high-temperature superconductors. Furthermore, the present Pb-Bi2201 system is in a heavily overdoped regime that is not accessible in the Bi2212-based system. Therefore, the influence of carriers on the inhomogeneity could be studied in greater detail.

Single crystals of Pb-Bi2201 were grown by the floating zone technique, similar to the method reported by another group.²⁶ The chemical composition, as determined by inductively coupled plasma (ICP) emission spectrometry, is $\text{Bi}_{1.83}\text{Pb}_{0.37}\text{Sr}_{1.91}\text{CuO}_y$. The as-grown crystals were postannealed under a vacuum at high temperature (500–600 °C). The superconducting transition temperature T_c of the annealed crystals was determined to be 10 K using a superconducting quantum interference device (SQUID) susceptometer.

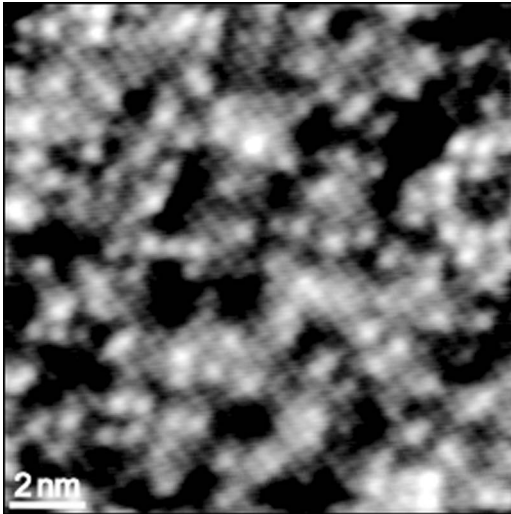


FIG. 1. Constant-current STM image observed on the cleaved *ab* surface of a Pb-Bi2201 single crystal at 4.5 K. The scanning area is 10×10 nm. The sample bias voltage and set-point current are $V_s = 110$ mV and $I_t = 0.35$ nA, respectively.

STM/STS measurements were carried out using an ultrahigh-vacuum low-temperature STM instrument equipped with a low-temperature cleavage stage. The base pressure of the STM chamber was maintained at less than 2.0×10^{-10} Torr during the measurements. All samples examined here were cleaved *in situ* at 77 K to avoid oxygen loss from sample surfaces. The STM tips used were made of a mechanically sharpened Pt-Ir alloy.

Figure 1 shows STM topographic images obtained on a cleaved *ab* surface of a Pb-Bi2201 crystal at 4.5 K. The figure clearly indicates a square lattice network of Bi atoms spaced 0.35 nm apart, which is comparable to the *a* axis or *b* axis length of the Pb-Bi2201 unit cell.²⁷ It can be seen that the present Pb-Bi2201 is free from modulations along the *b* axis, which is consistent with the results of electron diffraction measurements,²⁷ in contrast to Pb-Bi2212, in which the modulation structure persists up to $x \sim 0.4$.^{14,28} This suggests that Pb-Bi2201 contains more carriers than Pb-Bi2212 does at the same Pb content. In fact, recent photoemission measurements have revealed that the Fermi surface of Pb-Bi2201 is much larger than that of Pb-Bi2212.²⁹ We did not observe any sign of local phase separation into Pb-rich and Pb-poor regions, as seen in heavily Pb-doped Bi2212.^{14,15,28,30,31} In Fig. 1, some atomic sites show brighter contrast. These brighter spots represent approximately 16% of the Bi sites, which is in good agreement with the Pb content as revealed by ICP, namely 16.8%. Thus, we identify the spots as Pb atoms substituted into Bi sites.¹⁴ We have confirmed that such bright spots are not seen in the STM images of pure Bi2201.

Figure 2(a) is a spatial map of the superconducting gap value Δ . Values of Δ were deduced from conductance spectra as half the peak-to-peak energy separation. Notably, Δ shows a significant distribution, ranging from 13 to 30 meV, over the scanned area of 12.5×12.5 nm. We have checked that the tunneling barrier height ϕ is sufficiently high, ~ 3 eV, before and after the STS measurement, as shown in the inset

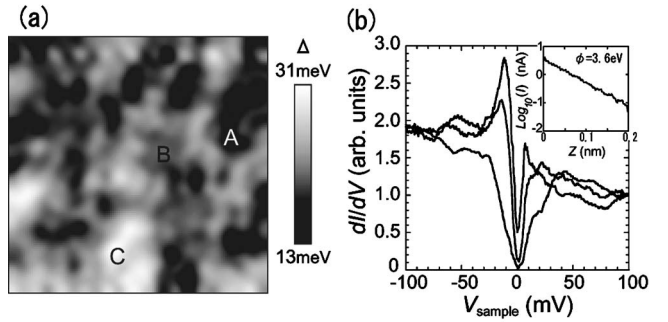


FIG. 2. (a) Δ distribution map observed on the cleaved *ab* surface of Pb-Bi2201 at 4.5 K. The scanning area is 12.5 nm \times 12.5 nm. (b) Tunneling spectra at points A, B, and C in (a). A typical z - $\log_{10}(I)$ curve is plotted in the inset.

of Fig. 2(b). This ensures that ideal vacuum tunneling is achieved. Similar gap inhomogeneity is reported in underdoped and optimally doped Bi2212 (Refs. 7–11) and Pb-doped Bi2212.^{14,15} The site-specified tunneling spectra observed at regions A, B, and C in Fig. 2(a) are plotted in Fig. 2(b). The tunneling spectrum A reveals well-developed conductance peaks superimposed on an inverse-V-shaped background, which has been argued to be a signature of the van Hove singularity. Furthermore, the Δ value estimated from spectrum A, 13 meV, is close to that reported for pure Bi2201 in the overdoped regime.³² Thus, we conclude that spectrum A represents a superconducting gap. In spectra B and C, on the other hand, the conductance peaks are substantially suppressed, and at the same time, the gap value Δ is enhanced. Particularly, spectrum C exhibits pseudogaplike behavior, characterized by large Δ up to 30 meV and dull gap edges. These findings clearly indicate that granular superconductivity is a commonly observed feature of Bi-based cuprates, regardless of the number of CuO_2 planes. Another remarkable feature seen in Fig. 2(b) is that the zero bias conductance increased with decreasing Δ . This suggests that local hole concentration is spatially nonuniform and elevated in smaller gap regions.¹⁸

Figures 3(a) and 3(b) compare a narrow-scan STM image and the corresponding Δ map, where open circles mark the locations of Pb atoms. There is clearly no correlation between the distributions of Δ and Pb. Therefore, we can conclude that the present electronic inhomogeneity is not a con-

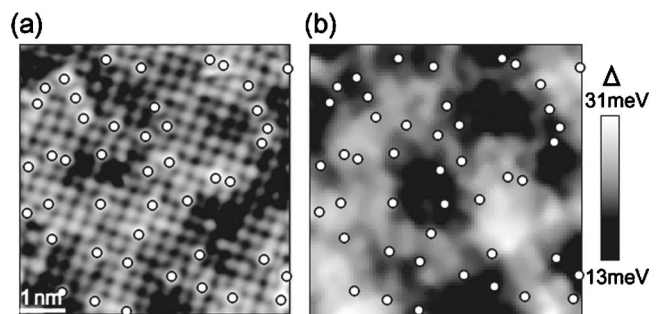


FIG. 3. Correlations between Pb distributions and Δ map in Pb-Bi2201 at 4.5 K. (a) STM image resolving Pb atoms; (b) the corresponding Δ map.

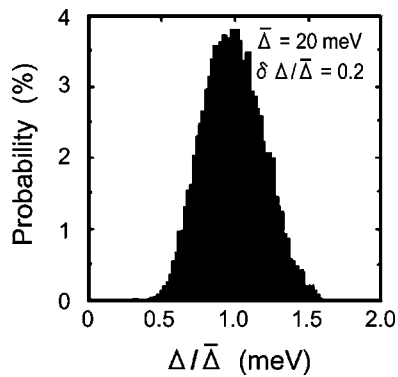


FIG. 4. Δ histogram of Pb-Bi2201.

sequence of Pb atoms randomly distributed in the surface BiO layer.¹⁴

Figure 4 shows a histogram of the gap value derived from the Δ map in Fig. 2. From Fig. 4, we evaluate the averaged value and standard deviation of Δ as $\bar{\Delta}=20$ meV and $\delta\Delta=4$ meV, respectively, yielding $\delta\Delta/\bar{\Delta}=0.2$. Interestingly, this ratio is close to that of slightly overdoped Bi2212 with $p=0.18$ holes per Cu atom, $\delta\Delta/\bar{\Delta}=0.22$.¹¹ Next, we compare the amount of excess oxygen in heavily overdoped Pb-Bi2201 and slightly overdoped Bi2212. Judging by the T_c value (~ 10 K), the former contains carriers of $p=0.4$,²⁹ from which the amount of excess oxygen d in the chemical formula $\text{Bi}_{1.83}\text{Pb}_{0.37}\text{Sr}_{1.91}\text{CuO}_{6+d}$ is estimated to be 0.225. In the case of the latter, d is evaluated to be 0.18 by assuming stoichiometric cation ratios, Bi: Sr: Ca: Cu=2:2:1:2. Thus, the two compounds have equivalent d values to within the uncertainty in the chemical composition of Bi2212,³³ despite the significant difference in carrier concentrations between

them. These results strongly suggest that electronic inhomogeneity is governed by the amount of excess oxygen, not the carrier concentration itself. This implies that the inhomogeneity is neither the signature of purely electronic phase separation³⁴ nor the inherent nature of Bi-based cuprates. According to a theoretical study based on a t - J model, electronic inhomogeneity is significantly affected by the spatial variation of local hole doping.¹⁸ Very recently, McElroy *et al.* reported atomic-scale impurity states located at $E=-0.96$ eV, whose densities are strongly correlated with the electronic inhomogeneity.¹⁷

It seems that the extent of electronic inhomogeneity, as expressed by $\delta\Delta/\bar{\Delta}$, is enhanced with increasing d . Indeed, Lang *et al.* reported $\delta\Delta/\bar{\Delta}=0.17$ and $\delta\Delta/\bar{\Delta}=0.22$ for underdoped ($p\approx 0.14$) and optimally+doped ($p\approx 0.18$) Bi2212.¹¹ However, this is not the case in the overdoped regime, where the ionic potential distribution becomes rather smooth with increasing d because the Coulomb potential curves associated with excess oxygen atoms overlap with each other. Therefore, it is anticipated that the extent of electronic inhomogeneity is suppressed with increasing d in overdoped samples. Indeed, Matsuda *et al.*¹⁶ reported that the Δ distribution profile becomes narrower, i.e., $\delta\Delta/\bar{\Delta}$ decreases, with d in overdoped Bi2212.

In summary, we have observed nanoscale electronic inhomogeneity comprising superconducting and pseudogap states in heavily overdoped Pb-Bi2201, using low temperature STM/STS. This leads to the conclusion that granular superconductivity is a general feature of Bi-based cuprates, regardless of the number of CuO_2 planes. The extent of the Δ distribution is comparable to those of pure Bi2212, suggesting that the electronic inhomogeneity is essentially independent of the carrier concentration itself, but rather, determined by the randomness of the excess oxygen distribution.

¹I. Maggio-Aprile, Ch. Renner, A. Erb, E. Walker, and Ø. Fischer, Phys. Rev. Lett. **75**, 2754 (1995).

²Ch. Renner, B. Revaz, K. Kadowaki, I. Maggio-Aprile, and Ø. Fischer, Phys. Rev. Lett. **80**, 3606 (1998).

³S. H. Pan, E. W. Hudson, A. K. Gupta, K.-W. Ng, H. Eisaki, S. Uchida, and J. C. Davis, Phys. Rev. Lett. **85**, 1536 (2000).

⁴S. H. Pan, E. W. Hudson, K. M. Lang, H. Eisaki, S. Uchida, and J. C. Davis, Nature (London) **403**, 746 (2000).

⁵W. E. Hudson, K. M. Lang, V. Madhavan, S. H. Pan, H. Eisaki, S. Uchida, and J. C. Davis, Nature (London) **411**, 920 (2001).

⁶G. Kinoda, H. Mashima, K. Shimizu, J. Shimoyama, K. Kishio, and T. Hasegawa, Phys. Rev. B **71**, 020502(R) (2005).

⁷T. Cren, D. Roditchev, W. Sacks, J. Klein, J.-B. Moussy, C. Deville-Cavellin, and M. Laguës, Phys. Rev. Lett. **84**, 147 (2000).

⁸T. Cren, D. Roditchev, W. Sacks, and J. Klein, Europhys. Lett. **54**, 84 (2001).

⁹C. Howald, P. Fournier, and A. Kapitulnik, Phys. Rev. B **64**, 100504(R) (2001).

¹⁰S. H. Pan, J. P. O'Neal, R. L. Badzey, C. Chamon, H. Ding, J. R. Engelbrecht, Z. Wang, H. Eisaki, S. Uchida, A. K. Gupta,

K.-W. Ng, E. W. Hudson, K. M. Lang, and J. C. Davis, Nature (London) **413**, 282 (2001).

¹¹K. M. Lang, V. Madhavan, J. E. Hoffman, E. W. Hudson, H. Eisaki, S. Uchida, and J. C. Davis, Nature (London) **415**, 412 (2002).

¹²K. McElroy, R. W. Simmonds, J. E. Hoffman, D.-H. Lee, J. Orenstein, H. Eisaki, S. Uchida, and J. C. Davis, Nature (London) **422**, 592 (2002).

¹³G. Kinoda, S. Nakao, T. Motohashi, Y. Nakayama, K. Shimizu, J. Shimoyama, K. Kishio, T. Hanaguri, K. Kitazawa, and T. Hasegawa, Physica C **388-389**, 273 (2003).

¹⁴G. Kinoda, T. Hasegawa, S. Nakao, T. Hanaguri, K. Kitazawa, K. Shimizu, J. Shimoyama, and K. Kishio, Phys. Rev. B **67**, 224509 (2003).

¹⁵G. Kinoda, T. Hasegawa, S. Nakao, T. Hanaguri, K. Kitazawa, K. Shimizu, J. Shimoyama, and K. Kishio, Appl. Phys. Lett. **83**, 1178 (2003).

¹⁶Azusa Matsuda, Takenori Fujii, and Takao Watanabe, Physica C **388-389**, 207 (2003).

¹⁷K. McElroy, Jinho Lee, J. A. Slezak, D.-H. Lee, H. Eisaki, S. Uchida, and J. C. Davis, Science **309**, 1048 (2005).

- ¹⁸Z. Wang, J. R. Engelbrecht, S. Wang, H. Ding, and S. H. Pan, *Phys. Rev. B* **65**, 064509 (2002).
- ¹⁹Y. N. Ovchinnikov, S. A. Wolf, and V. Z. Kresin, *Phys. Rev. B* **63**, 064524 (2001).
- ²⁰Q. H. Wang, J. H. Han, and D. H. Lee, *Phys. Rev. B* **65**, 054501 (2001).
- ²¹I. Martin and A. V. Balatsky, *Physica C* **357-360**, 46 (2001).
- ²²W. A. Atkinson, *Phys. Rev. B* **71**, 024516 (2005).
- ²³G. Kinoda, T. Yamanouchi, J. Kasai, T. Endo, X. Zhao, K. Kitazawa, and T. Hasegawa, *Physica C* **353**, 297 (2001).
- ²⁴M. Nishiyama, G. Kinoda, S. Shibata, T. Hasegawa, N. Koshizuka, and M. Murakami, *J. Supercond.* **15**, 351 (2002).
- ²⁵B. W. Hoogenboom, K. Kadowaki, B. Revaz, and Ø. Fischer, *Physica C* **391**, 376 (2003).
- ²⁶I. Chong, T. Terashima, Y. Bando, M. Takano, and Y. Matsuda, *Physica C* **290**, 57 (1997).
- ²⁷T. Terashima, I. Chong, Y. Bando, M. Takano, Y. Matsuda, T. Nagaoka, and K.-I. Kumagai, *Physica C* **282-287**, 57 (1997).
- ²⁸T. Motohashi, Y. Nakayama, T. Fujita, K. Kitazawa, J. Shimoyama, and K. Kishio, *Phys. Rev. B* **59**, 14080 (1999).
- ²⁹T. Kondo, T. Takeuchi, T. Yokoya, S. Tsuda, S. Shin, and U. Mizutani, *J. Electron Spectrosc. Relat. Phenom.* **137-140** 663 (2004).
- ³⁰I. Chong, Z. Hiroi, J. Shimoyama, Y. Nakayama, K. Kishio, T. Terashima, Y. Bando, and M. Takano, *Science* **276**, 770 (1997).
- ³¹S. Nakao, K. Ueno, T. Hanaguri, K. Kitazawa, T. Fujita, Y. Nakayama, T. Motohashi, J. Shimoyama, K. Kishio, and T. Hasegawa, *J. Low Temp. Phys.* **117**, 341 (1999).
- ³²M. Kugler, Ø. Fischer, Ch. Renner, S. Ono, and Y. Ando, *Phys. Rev. Lett.* **86**, 4911 (2001).
- ³³H. Eisaki, N. Kaneko, D. L. Feng, A. Damascelli, P. K. Mang, K. M. Shen, Z.-X. Shen, and M. Greven, *Phys. Rev. B* **69**, 064512 (2004).
- ³⁴J. C. Phillips, A. Saxena, and A. R. Bishop, *Rep. Prog. Phys.* **66**, 2111 (2003).